Radiation effects on MOS and bipolar devices by 8 MeV protons, 60 MeV Br ions and 1 MeV electrons*

Li Xing-Ji(李兴冀)[a)†], Geng Hong-Bin(耿洪滨)[a)], Lan Mu-Jie(兰慕杰)[b)],
Yang De-Zhuang(杨德庄)[a)], He Shi-Yu(何世禹)[a)], and Liu Chao-Ming(刘超铭)[a)]

[a)] *Space Materials & Environment Engineering Laboratory, Harbin Institute of Technology, Harbin* 150001, *China*
[b)] *School of Astronautics, Harbin Institute of Technology, Harbin* 150001, *China*

(Received 20 July 2009; revised manuscript received 9 October 2009)

The radiation effects of the metal-oxide-semiconductor (MOS) and the bipolar devices are characterised using 8 MeV protons, 60 MeV Br ions and 1 MeV electrons. Key parameters are measured *in-situ* and compared for the devices. The ionising and nonionising energy losses of incident particles are calculated using the Geant4 and the stopping and range of ions in matter code. The results of the experiment and energy loss calculation for different particles show that different incident particles may give different contributions to MOS and bipolar devices. The irradiation particles, which cause a larger displacement dose within the same chip depth of bipolar devices at a given total dose, would generate more severe damage to the voltage parameters of the bipolar devices. On the contrary, the irradiation particles, which cause larger ionising damage in the gate oxide, would generate more severe damage to MOS devices. In this investigation, we attempt to analyse the sensitivity to radiation damage of the different parameter of the MOS and bipolar devices by comparing the irradiation experimental data and the calculated results using Geant4 and SRIM code.

Keywords: radiation effects, MOS and bipolar devices, ionisation damage, displacement damage
PACC: 6180, 8750G, 7340Q, 7340L

1. Introduction

In orbit, exposure to high fluxes of electrons and protons can significantly reduce spacecraft lifetime due to total dose effects.[1−3] For years, investigators performing radiation tests on metal-oxide-semiconductor (MOS) and bipolar devices destined for use in spacecraft have relied primarily on Co-60 generated gamma rays to simulate the natural space radiation environment. A possible problem with this simulation method is that the natural space radiation environment consists mainly of high energy protons and electrons, but does not consist of Co-60 gamma rays.[4] The MOS and bipolar devices are two basic types of Si-based ones. It is of significance to properly understand the radiation damage in the two types of devices, which will help to clarify the difference in radiation effects caused by different charged particles.

MOS devices may be susceptive to ionisation damage, and the most sensitive part of the MOS devices to radiation is the oxide insulator.[5] When incident particles pass through a gate oxide, electron/hole pairs (ehps) are created by the deposited energy. In SiO_2, the electrons are much more mobile than the holes,[6] and they are swept out of the oxide, typically in a picosecond or less. However, at the same time, some fraction of the electrons and holes will be recombined. The fraction will depend greatly on the energy and type of the incident particles, such as 8 MeV protons, 60 MeV Br ions and 1 MeV electrons. The number of the holes, which escape from the initial recombination, influences the capability of the MOS devices. The comparison of radiation effects on the MOS devices caused by Co-60 gamma rays, protons and electrons was investigated in the past years,[4,7,8] but there is little analysis related to the radiation damage on MOS devices produced by Br ions, which would produce more displacement damage.

Unlike MOS devices, bipolar devices may be susceptive to both ionisation damage and displacement damage. Bipolar devices contain insulators on the surface and Si bulk. Three basic processes could occur: (1) inversion at the surface, which occurs because of charge trapping in the insulator, (2) changes in the surface recombination rate of minority carriers, and (3) bulk damage.[9] The processes (1) and (2) are related to the ionisation damage and the bulk damage to the displacement damage. Different incident charged particles, may contribute to the ionisation or displacement damage differently, especially the heavy

*Project supported by the National Basis Research Program of China (Grant No. 61343).
†Corresponding author. E-mail: lxj0218@tom.com
© 2010 Chinese Physical Society and IOP Publishing Ltd

ions, but such investigations are few.[10−12]

The objective of this investigation is to examine the irradiation effects on the electrical behaviour of the MOS and the bipolar devices caused by protons, electrons and Br ions under various dose levels. An attempt is made to explain the radiation-induced degradation of MOS and bipolar devices, based on calculations of the total ionising dose $D_{\rm i}$ and displacement dose $D_{\rm d}$ calculated using the Geant4 and the stopping and range of ions in matter (SRIM).

2. Calculation of ionising and nonionising doses

The use of rad-hard MOS and bipolar devices in spacecraft for missions of long duration is increasing. The rad-hard complementary metal-oxide-semiconductor (CMOS) devices of CC4013 type and transister-transister-logic (TTL) devices of 54LS86 type are chosen as samples. The sensitive region of the devices to the radiation effects must be analysed before calculating the ionising and nonionising doses.

Figure 1 shows the lengthways structure of the CC4013 devices. The sensitive region of the CC4013 devices to radiation effects (ionisation effects) is the gate oxide, so that the projection range of incident particles for the irradiation experiment must preponderate over the location of the sensitive region. The insulator thickness is about 500 nm, the thicknesses of Aluminium and the gate oxide are about 1.2 μm and 50 nm, respectively.

Figure 2 shows the lengthways structure of the 54LS86 devices. The sensitive region of the 54LS86 device to radiation effects (ionisation and displacement effects) are both the Si bulk and the insulators. The projection range of incident particles for the irradiation experiment must preponderate over the location of the p-Si region. The thicknesses of insulator aluminium and the p-Si region are about 1.5 μm, 1.6 μm and 1.5 μm, respectively. Therefore, the projection range of incident particles must be longer than 3.0 μm.

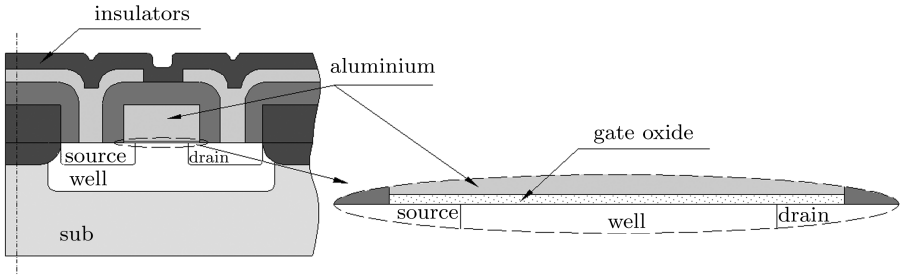


Fig. 1. The lengthways structure of the CC4013 device.

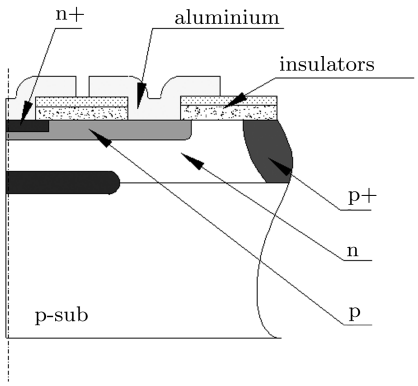


Fig. 2. The lengthways structure of the 54LS86 device.

The ionising absorbed dose $D_{\rm i}$ and nonionising absorbed dose (displacement absorbed dose) $D_{\rm d}$ produced by monoenergetic charged particles irradiation can be calculated by following equations:

$$D_{\rm i}(t) = 1.6 \times 10^{-8} \times {\rm LET}(t) \times \Phi, \quad (1)$$

$$D_{\rm d}(t) = 1.6 \times 10^{-8} \times {\rm NIEL}(t) \times \Phi, \quad (2)$$

where, $D_{\rm i}(t)$ and $D_{\rm d}(t)$ are the ionising absorbed dose and displacement absorbed dose as a function of depth in chip material of the devices, the unit is rad; t is the depth of device chips, the unit is μm; 1.6×10^{-8} is the unit conversion parameter, the unit is rad·g/MeV; Φ is the fluence of the incident particles, the unit is p/cm^2 for protons, e$^-$/cm^2 for electrons and ion/cm^2 for heavy ions; LET(t) and NIEL(t) are the ionising and nonionising energy losses as a function of depth

in chip material of devices and could be calculated by the Monte Carlo code Geant4 and SRIM, the unit is MeV·cm^2/g.

The ionising and nonionising absorbed dose in device chips produced by both electrons and protons are calculated using the Geant4 code. The ionising and nonionising absorbed doses in device chips produced by Br ions were calculated using the SRIM code. The ionising dose in device chips produced by Br ions could also be calculated using Geant4, and by which the calculated result corresponds well with the SRIM. But the nonionising dose produced by Br ions is difficultly calculated using the Geant4.

The ionising doses per unit fluence of the protons, electrons and Br ions are plotted as a function of the chip depth of CC4013 device in Fig. 3, and in Fig. 4 the results are for 54LS86 device, based on the values of the LET calculated by Geant4 and SRIM. We could know per unit fluence of Br ions have stronger capability of ionisation than both protons and electrons in the same depth, as shown in Figs. 3 and 4.

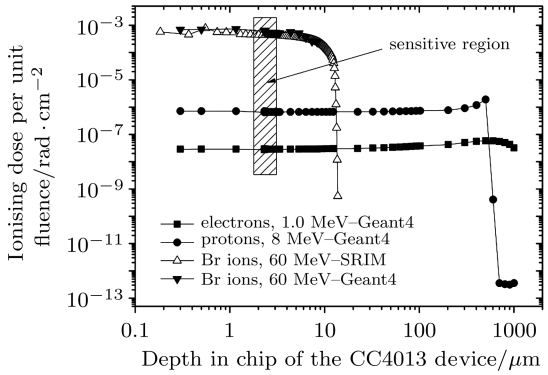


Fig. 3. The ionising dose per unit fluence as a function of the CC4013 device chip. The ionising doses were calculated by Geant4 for electrons and protons, and calculated by both Geant4 and SRIM for Br ions.

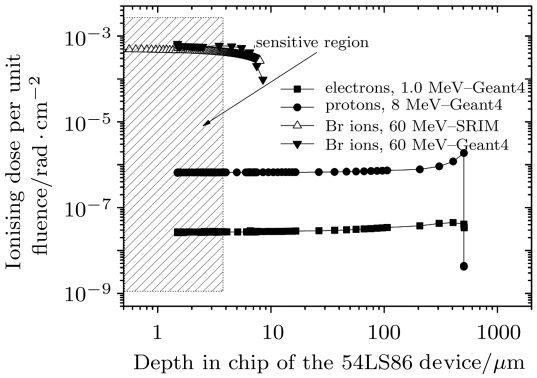


Fig. 4. The ionising dose per unit fluence as a function of the 54LS86 device chip. The ionising doses were calculated by Geant4 for electrons and protons, and calculated by both Geant4 and SRIM for Br ions.

The nonionising doses per unit fluence of the protons, electrons and Br ions are plotted as a function of the chip depth of the CC4013 device and 54LS86 device in Figs. 5 and 6, based on the values of the NIEL calculated by Geant4 and SRIM. It could be known that unit fluence of Br ions has stronger capability of nonionising than those for both protons and electrons in the same depth, as shown in Figs. 5 and 6.

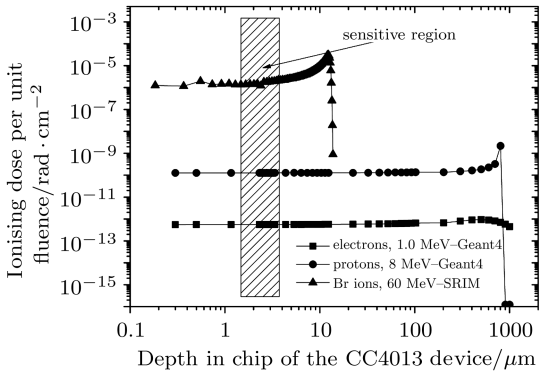


Fig. 5. The nonionising dose per unit fluence as a function of the CC4013 device chip. The nonionising doses were calculated by Geant4 for electrons and protons, and calculated by SRIM for Br ions.

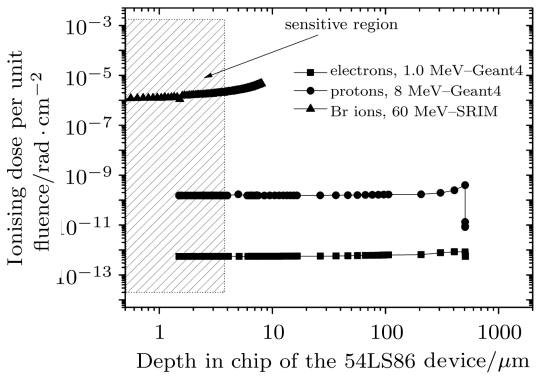


Fig. 6. The nonionising dose per unit fluence as a function of the 54LS86 device chip. The nonionising doses were calculated by Geant4 for electrons and protons, and calculated by SRIM for Br ions.

From Fig. 3 to Fig. 6, it could be seen the ionising dose is over two, three and four orders of magnitude more than the nonionising doses for Br ions, protons and electrons, respectively. The Br ions have the maximal capability of ionising, on the contrary, the electrons have minimal capability of nonionising. The results from Fig. 3 to Fig. 6 show that nonionising dose is much less than ionising dose, and heavier particles contribute more to nonionising dose, which is consistent with the Lindhard–Scharff–Schiott theory.

3. Experimental details

3.1. Samples and test conditions

The objective of this investigation is to examine the radiation response of the MOS devices and bipolar devices irradiated by protons, electrons, and Br ions; then, from the results, to determine the difference in the susceptivity to ionisation and nonionisation damage caused by different charged particles. To accomplish this task, large numbers of rad-hard CC4013 devices and 54LS86 devices were used to be irradiated, including CMOS Al-gate 4013 triggers and the TTL 54LS86. The gate oxide of the CC4013 is SiO_2 with the thickness of 50 nm. The thicknesses are about 1.2 μm and 500 nm for the Al-gate and insulators on the chip surface of CC4013 device, respectively. The thicknesses are 1.6 μm and 1.5 μm for the Al downlead and insulators on the chip surface of 54LS86 device, respectively. Uncertainties of measured parameters are less than 5 percent.

The CMOS and TTL devices were unbiased during irradiation, and measured with different test conditions for different parameters, processed under MIL-STD-883G specifications. Device parameters were measured *in-situ* using a semiconductor parameter measurement systems, which consists of KEITHLEY 4200-SCS and AGILENT E4980A performed within 5 minutes during irradiation for charged particles. Turn-around time between irradiation and device measurement was maintained at approximately 5 seconds or less. All irradiations and measurements were performed at room temperature, and all of the samples were decapped.

A matrix board switching system located outside of the irradiation chamber was used as a naster control panel. The board interfaces up to four devices under test (DUT) with the power supplies and measurement equipment, as shown in Fig. 7. The matrix board was designed to have very high insulation resistance so that extremely low current could be generated.



Fig. 7. The photo of connecting board containing four DUTs.

3.2. Irradiation sources and procedures

The test facilities used in this investigation are the EN Tandem Accelerator in State Key Laboratory of Nuclear Physics and Technology, Peking University, China for protons and Br ions; High Frequency High Voltage Electron Accelerator in the Technical Physical Institute of Heilongjiang Academy of Science, China for electrons. The proton and Br ion tests were conducted in a vacuum chamber with Faraday cup dosimeter. Electron exposures were performed in local atmospheric conditions.

Beam area of protons, electrons and Br ions were defined, and held constantly. To ensure accuracy, beam uniformity was monitored during the irradiation. Then the fluence of the protons, electrons and Br ions could be confirmed by the beam area and the current measured by the Faraday cup. And the total dose in CC4013 and 54LS86 devices could be calculated using the Eqs. (1) and (2).

4. Experimental results

Figure 8 shows that the p-channel threshold voltage shifts with the total dose of the rad-hard CC4013 devices. The irradiation sources were 8 MeV protons, 1 MeV electrons, and 60 MeV Br ions. The irradiation fluxes for 8 MeV protons, 1 MeV electrons and 60 MeV Br ions are 1.66×10^9 p/cm$^2 \cdot$s^{-1}, 2.53×10^{11} e$^-$/cm$^2 \cdot$s^{-1} and 7.12×10^7 ions/cm$^2 \cdot$s^{-1}, respectively. Test condition of p-channel threshold voltage for the CC4013 devices is given in Fig. 8.

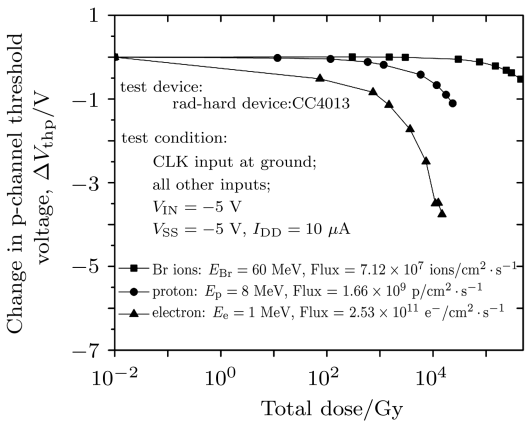


Fig. 8. The change in p-channel threshold voltage as a function of total dose in CC4013 device chip.

Figure 9 shows that the n-channel threshold voltage shifts with the total dose of the rad-hard CC4013 devices. The irradiation condition and test condition for n-channel threshold voltage is given Fig. 9.

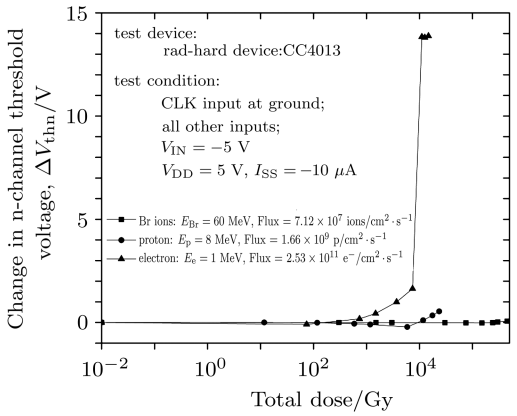


Fig. 9. The change in n-channel threshold voltage as a function of the total dose in CC4013 device chip.

It is noted that the data for 8 MeV protons, 1 MeV electrons and 60 MeV Br ions do not track with each other under the same test condition for both p-channel and n-channel threshold voltage shifts. The change in the p-channel and n-channel threshold voltage in the CC4013 devices for Br ions is smaller than that for other particles. Such a result might be attributed to the larger ionising energy loss for the Br ions to traverse through the silicon dioxide (approximately 0.5 μm) and aluminum (approximately 1.2 μm) layers of the test samples. The incident particles giving higher ionising energy loss could induce higher recombination rates for the ehps caused by ionisation in the gate oxide (SiO_2), producing lower radiation-induce degradation of the threshold voltage.

Figure 10 shows the change in input clamp voltage as a function of total dose for the rad-hard 54LS86 devices. The irradiation sources were 8 MeV protons, 1 MeV electrons, and 60 MeV Br ions. The average irradiation fluxes for 8 MeV protons and 60 MeV Br ions are 1.12×10^9 p/cm$^2 \cdot$s^{-1} and 8.60×10^7 ions/cm$^2 \cdot$s^{-1}, respectively. The irradiation fluxes of 1 MeV electrons are 2.79×10^{11} and 1.58×10^{12} e$^-$/cm$^2\cdot$s^{-1}. The test condition for the input clamp voltage is given in Fig. 10.

The data for protons, electrons, and Br ions do not track with each other under the same test condition for the change in input clamp voltage, especially for the high flux (1.58×10^{12} e$^-$/cm$^2 \cdot$s^{-1}) and low flux irradiation electrons (2.79×10^{11} e$^-$/cm$^2 \cdot$s^{-1}). Change in the input clamp voltage produced by low flux electrons is lower than that for high flux electrons. Being contrary to the CC4013 devices, Br ions can give most largest contribution to the change in input clamp voltage of the 54LS86 devices. This phenomenon can be attributed to the susceptivity to displacement damage for the bipolar devices, because the Br ions could produce the most nonionising damage than the others.

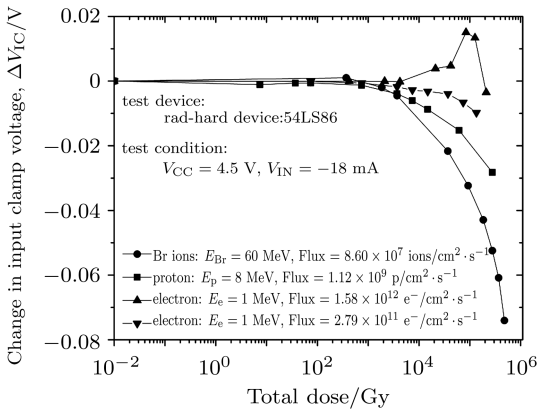


Fig. 10. The change in input clamp voltage as a function of the total dose for 54LS86 device.

The change in low level supply current as a function of total dose for the rad-hard 54LS86 devices is shown in Fig. 11 where the irradiation and test conditions are given. The results in Fig. 11 show that the data for protons, electrons, and Br ions does not track with each other under the same test condition for the change in low level supply current. Unlike V_{IC}, the change in low-level supply current I_{CCL} of the 54LS86 devices is not distinctly influenced by the flux of the electrons. The most distinction between the change in V_{IC} and I_{CCL} can be related to the susceptivity to radiation effects. V_{IC} is much more susceptive to displacement damage, whereas I_{CCL} is much more susceptive to ionisation damage. The influence of radiation damage on the change in I_{CCL} of TTL 54LS86

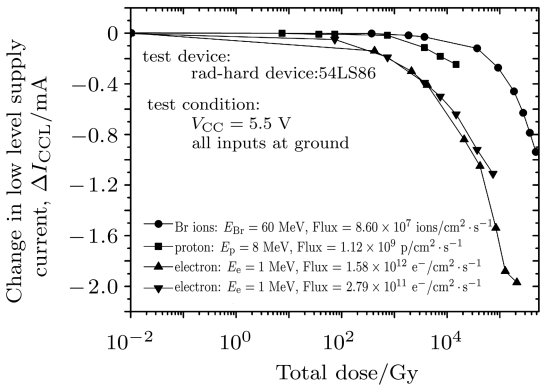


Fig. 11. The change in low level supply current as a function of the total dose for 54LS86 device.

devices is similar to that on the change in the threshold voltage of CMOS CC4013 device for protons, electrons, and Br ions.

5. Discussion

5.1. Irradiation source influence on MOS devices

The results given in Figs. 8 and 9 show that the damage produced by protons and Br ions in the CMOS devices is always less than that by electrons. An explanation for the above results might be that the ionisation capability is discrepant for different particles irradiations, and that MOS devices are susceptive to the particles that produced severe ionising damage. The ionisation damage, proportional to ionising dose, is mainly lead by the trapped holes in the gate oxide and the interface traps, which is generated by charged particles.

The physical processes that lead to the creation of ionisation damage are: 1) the generation of ehps, 2) the prompt recombination of a fraction of the generated ehps, 3) the transport of free carriers remaining in the oxide, and either 4a) the formation of trapped charge via hole trapping in defect precursor sites or 4b) the formation of interface traps via reactions involving hydrogen.[13−15]

Once generated, a fraction of the ehps is annihilated through either columnar or geminate recombination (process 2). The ehps that escape this initial recombination process divided by total ehps generated is the fractional charge yield. Figure 12 plots the fractional yield of holes generated in SiO_2 as a function of the radiation type.[1,5] The figure also indicates that electron-hole pair recombination is a function of the electric field within the material.[16] It is believed that electrons, having a much higher mobility than holes in oxides, could rapidly be swept out of the dielectric. The surviving holes will undergo polaron hopping transport via shallow traps in the SiO_2 (process 3). A fraction of these transporting holes may fall into deep traps in the oxide bulk or near the Si/SiO_2 interfaces, forming trapped positive charge (process 4a). The hole trapping efficiency is also a function of the electric field in the oxide. The trapped hole defect may, depending on their proximity to the interfaces, exchange charges with the underlying Si via electron tunneling.[17] Reactions between holes and hydrogen-containing defects or dopant complexes can also lead to the formation of a second type of ionisation defects: the interface trap (process 4b).[18]

A high LET particle or high ionising dose per unit fluence will deposit more charges than a low LET one. The surviving fraction is lower for a high LET particle or high ionising dose per unit fluence. The total amount of charge per particle is proportional to the multiplication of charge yield by surviving fraction. The ionisation damage to MOS devices might be determined by the initial charge yield. Reference [19] believed that the initial charge yield would vary inversely with ionising stopping power.

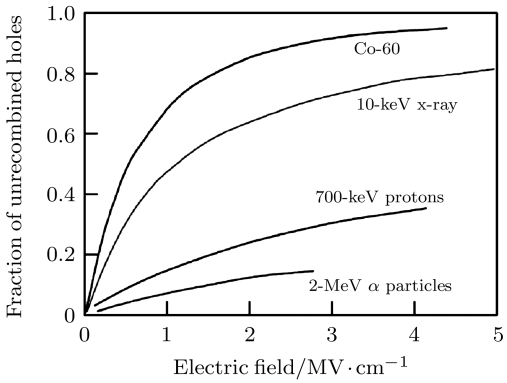


Fig. 12. Fractional yield of holes generated in SiO_2 as a function of electric field in the material.[1,5]

From the results in Figs. 3 and 8, a conclusion, which is in agreement with the summing-up in Ref. [19], could be putatively drawn that high ionising dose per unit fluence or high LET particles in the same depth for charged particles will lead to high initial ehps recombination rates and low initial charge yields, which produce low ionising damage to the MOS devices; conversely, for low ionising dose per unit fluence or low LET particles, the generated electron-hole pairs will be farther apart, leading to lower initial recombination rates and higher initial charge yields, which produce bigger ionising damage to the MOS devices.

The results in Fig. 9 show the large positive n-channel threshold voltage shifts mainly caused by the interface traps, because the positive oxide trapped charge would give a negative shift. From the results in Figs. 3 and 9, a conclusion could be putatively that the amount of the interface traps would be inverse proportion to the ionising dose per unit fluence of charged particles.

Compared the results in Fig. 3 with Figs. 8 and 9, a conclusion could be putatively that the bigger the ionising dose per unit fluence or the LET of charged

particles in the chip sensitive regions, the lower the ionisation damage to the MOS devices.

5.2. Irradiation source influence on bipolar devices

Figure 10 illustrates the damage produced by Br ions which is higher than that by the others in the bipolar devices. One can conclude from the results in Fig. 10 that the damage sensitivity increases from the 1 MeV electrons to 60 MeV Br ions, coordinative to the results in Fig. 6. The nonionisation dose per unit fluence in Fig. 6 is increased from the 1 MeV electrons to 60 MeV Br ions. For the high flux electron irradiation, the change in $V_{\rm IC}$ is different from that for other particles, which may be influenced by the inner structure of the bipolar devices. Therefore, it is unbefitting to select the high flux electrons for irradiation experiment. It could be concluded that the voltage of the bipolar devices is more sensitive to the displacement damage based on the results in Figs. 6 and 10.

The change in low level supply current produced by Br ions is lower than those by other particles as shown in Fig. 11, which is opposite to the change in voltage parameter of the TTL devices and similar to the MOS devices. Therefore, it could be concluded that the current of the bipolar devices is more sensitive to the ionisation damage based on the results in Figs. 4 and 11. Extensive work has been done on ionising radiation effects in the MOS devices. In contrast, little work has been related to the bipolar devices. The oxides in the bipolar structure are similar to MOS field oxides, and hence their radiation effects could be similar, although the lateral fringing fields in bipolar devices are lower in magnitude than fringing fields in MOS field oxides.

To sum up, the parameter of the bipolar devices may be susceptive to ionisation damage or displacement damage. For example, the $V_{\rm IC}$ of TTL 54LS86 devices is susceptive to displacement damage, while the $I_{\rm CCL}$ of the TTL 54LS86 devices susceptive to ionisation damage. Thus the bipolar devices could be susceptive to both ionisation and displacement damage due to different damage mechanisms, which is different to the MOS devices.

6. Conclusions

The calculated results of ionisation and displacement dose by Geant4 and SRIM could be used to analyse the experimental results for both MOS and bipolar devices. The damage sensitivities of the MOS and bipolar devices depend on irradiation source types (electrons, protons, and Br ions) and energies. For the MOS devices tested, the radiation damage produced by 1 MeV electrons is greater than the damage produced by 8 MeV protons or 60 MeV Br ions, which could show that the bigger the ionising dose per unit fluence of charged particles in the chip sensitive regions, the lower the ionisation damage to the MOS devices. The voltage parameters of the bipolar devices are susceptive to displacement damage, while current parameters of the bipolar devices are susceptive to the ionising damage, both of which could be well understood by the experimental data and the calculated results of 8 MeV protons, 60 MeV Br ions and 1 MeV electrons.

References

[1] Schwank J R, Shaneyfelt M R, Fleetwood D M, Felix J A, Dodd P E, Paillet P and Ferlet-Cavrois V 2008 *IEEE Trans. Nucl. Sci.* **55** 1833

[2] Zhang C X, Tian H T, Li M, Jin J and Song N F 2008 *Chin. Phys.* B **17** 573

[3] Zhang L, Zhang Y M, Zhang Y M, Han C and Ma Y J 2009 *Chin. Phys.* B **18** 3490

[4] Tallon R W, Ackermann M R, Kemp W T, Owen M H and Saunders D P 1985 *IEEE Trans. Nucl. Sci.* **NS-32** 4393

[5] Oldham T R and McLean F B 2003 *IEEE Trans. Nucl. Sci.* **50** 486

[6] Hughes R C 1973 *Phys. Rev. Lett.* **30** 1333

[7] Gauthier M K and Nichols D K 1983 *IEEE Trans. Nucl. Sci.* **NS-30** 4192

[8] He B P, Chen W and Wang G Z 2006 *Acta Phys. Sin.* **55** 3546 (in Chinese)

[9] Johnston A H, Swift G M and Rax B G 1994 *IEEE Trans. Nucl. Sci.* **41** 2427

[10] Kulkarni S R, Ravindra M, Joshi G R and Damle R 2006 *Nucl. Instrum. Meth.* B **251** 157

[11] Gnana Prakash A P, Ke S C and Siddappa K 2004 *Nucl. Instrum. Meth.* B **215** 457

[12] Dinesh C M, Ramani, Radhakrishna M C, Dutt R N, Khan S A and Kanjilal D 2008 *Nucl. Instrum. Meth.* B **266** 1713

[13] Chen W H, Du L, Zhuang Y Q, Bao J L, He L, Zhang T F and Zhang X 2009 *Acta Phys. Sin.* **58** 4090 (in Chinese)

[14] Li D M, Wang Zh H, Huang L Y and Gou Q J 2007 *Chin. Phys.* **16** 3760
[15] Barnaby H J 2006 *IEEE Trans. Nucl. Sci.* **53** 3103
[16] Shaneyfelt M R, Schwank J R, Fleetwood D M, Winokur P S, Hughes K L and Sexton F W 1990 *IEEE Trans. Nucl. Sci.* **37** 1632
[17] Fleetwood D M 1996 *IEEE Trans. Nucl. Sci.* **43** 779
[18] Tsetseris L, Schrimpf R D, Fleetwood D M, Pease R L and Pantelides S T 2005 *IEEE Trans. Nucl. Sci.* **52** 2265
[19] Paillet P, Schwank J R, Shaneyfelt M R, Ferlet-Cavrois V, Jones R L, Flament O and Blackmore E W 2002 *IEEE Trans. Nucl. Sci.* **49** 2656